Role of Water in Mediating the Assembly of Alzheimer Amyloid-beta Aβ16-22 Protofilaments

Supplemental Information

Mary Griffin Krone, Lan Hua, Patricia Soto, Ruhong Zhou, B.J. Berne and Joan-Emma Shea

Figure 6: Animated GIF movie depicting MD trajectory of two un-constrained peptide layers using the full potential energy function. For clarity, only water molecues between the layers are shown. This trajectory corresponds to Fig. 2b-i of the main text.

Figure 7: Animated GIF movie depicting MD trajectory of two un-constrained peptide layers when van der Waals attractions are turned off. For clarity, only water molecues between the layers are shown. This trajectory corresponds to Fig. 8b of the supplemental information.

Figure 8: (a) Plots of the number of water molecules between the two 9-stranded peptide sheets as a function of time for the positionally restrained wetting and dewetting simulations at 300K in which the protein-water van der Walls attraction is turned off (λ^a=0). In the dewetting simulations (red curve), the peptides were solvated and minimized followed by the addition of position restraints on the peptides. The black curve represents the wetting simulations in which all water molecules were removed from the interior of the peptide sheets after solvation and minimization and prior to positionally restrained simulation. From these plots, the dewetting critical distance, D_c, is found to be approximately 2.58nm. In simulations at and below D_c a complete drying of the interior region is observed, in contrast to the simulations shown in Fig. 2a. (b-top) Plots of the number of water molecules between the peptide sheets as a function of time for un-constrained MD simulations in which the protein-water van der Walls attraction is turned off. Each plot shows a different trajectory starting from an initial inter-sheet separation, D_0, of 2.38nm. (b-bottom) Plots of the center of mass distance between the two peptide sheets as a function of time for un-constrained MD simulations in which the protein-water van der Walls attraction is turned off. Each plot corresponds to the same trajectory as the plot above it. Although a lag phase appears prior to the β-sheet association, once the association is initiated, the timescale of association is much faster than when the full potential is used.

Figure 9: (a-h)The number of inter-peptide water molecules is plotted against the inter-peptide distance for 8 separate trajectories at 300K where D_0=1.28nm. Trajectories a-e do not appear to show a dewetting transition while trajectories f-h do. (i-p) The number of inter-peptide water

molecules is plotted against the inter-peptide distance for 8 separate trajectories at 300K, with no peptide-water van der Waals attraction, where D_0=2.38nm. Each simulation shows a strong dewetting transition. (q-x) The number of inter-peptide water molecules is plotted against the inter-peptide distance for 8 separate trajectories at 300K, with no peptide-water Electrostatic interaction, where D_0=1.28nm. Trajectories q-u do not appear to show a dewetting transition while trajectories v-x do.

Figure 10: (a-b) Two separate simulations are shown in which both the protein-water van der Waals attraction and repulsion are scaled by a factor of λ^a and λ^r, respectively and $\lambda^a = \lambda^r$. Similar to the results shown in Fig. 4 a-b of the main text, a dewetting transition occurs approximately when $\lambda^a = \lambda^r$=0.8. In contrast to simulations in which only the protein-water van der Waals attraction is nearly turned off (λ^a =0.05 in Fig. 4a-b), when the repulsion is nearly turned off, the sheets do not collapse and a complete drying is not observed. We speculate that when there is almost no protein-water van der Waals repulsion, there are no significant forces driving the water away from the protein, and the volume the water occupies is significant enough to prevent drying.

Figure 6: (movie file)
(see mpg file:Figure6S.mpg)
Figure 7: (movie file)
(see mpg file:Figure7S.mpg)

Figure 8:

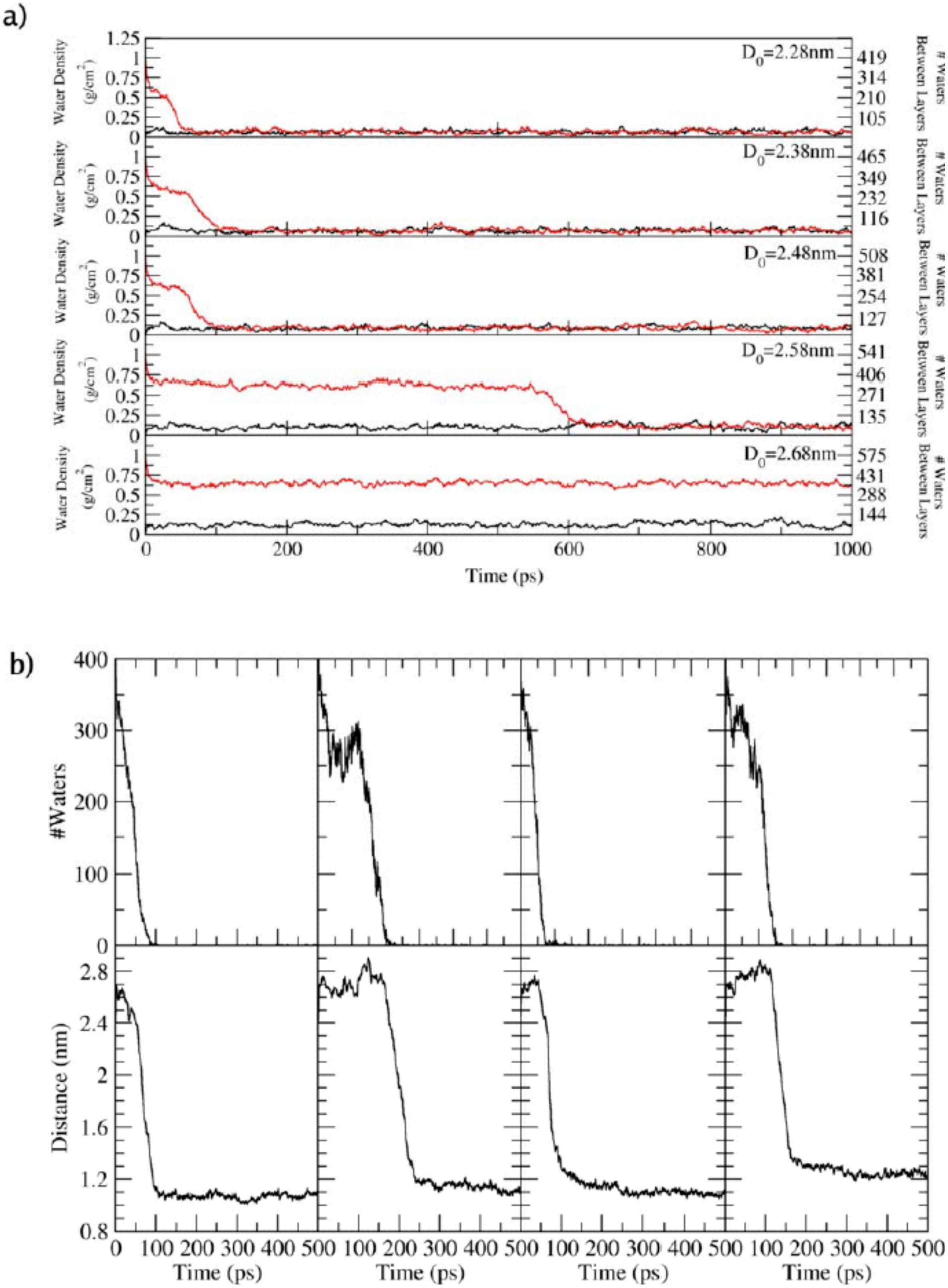
a)
Water Density (g/cm^2)
Waters Between Layers
1.25
1
0.75
0.5
0.25
0
D$_0$=2.28nm
419
314
210
105
D$_0$=2.38nm
465
349
232
116
D$_0$=2.48nm
508
381
254
127
D$_0$=2.58nm
541
406
271
135
D$_0$=2.68nm
575
431
288
144
0
200
400
600
800
1000
Time (ps)
b)
#Waters
400
300
200
100
0
Distance (nm)
2.8
2.4
2
1.6
1.2
0.8
0 100 200 300 400 500
Time (ps)

Figure 9:

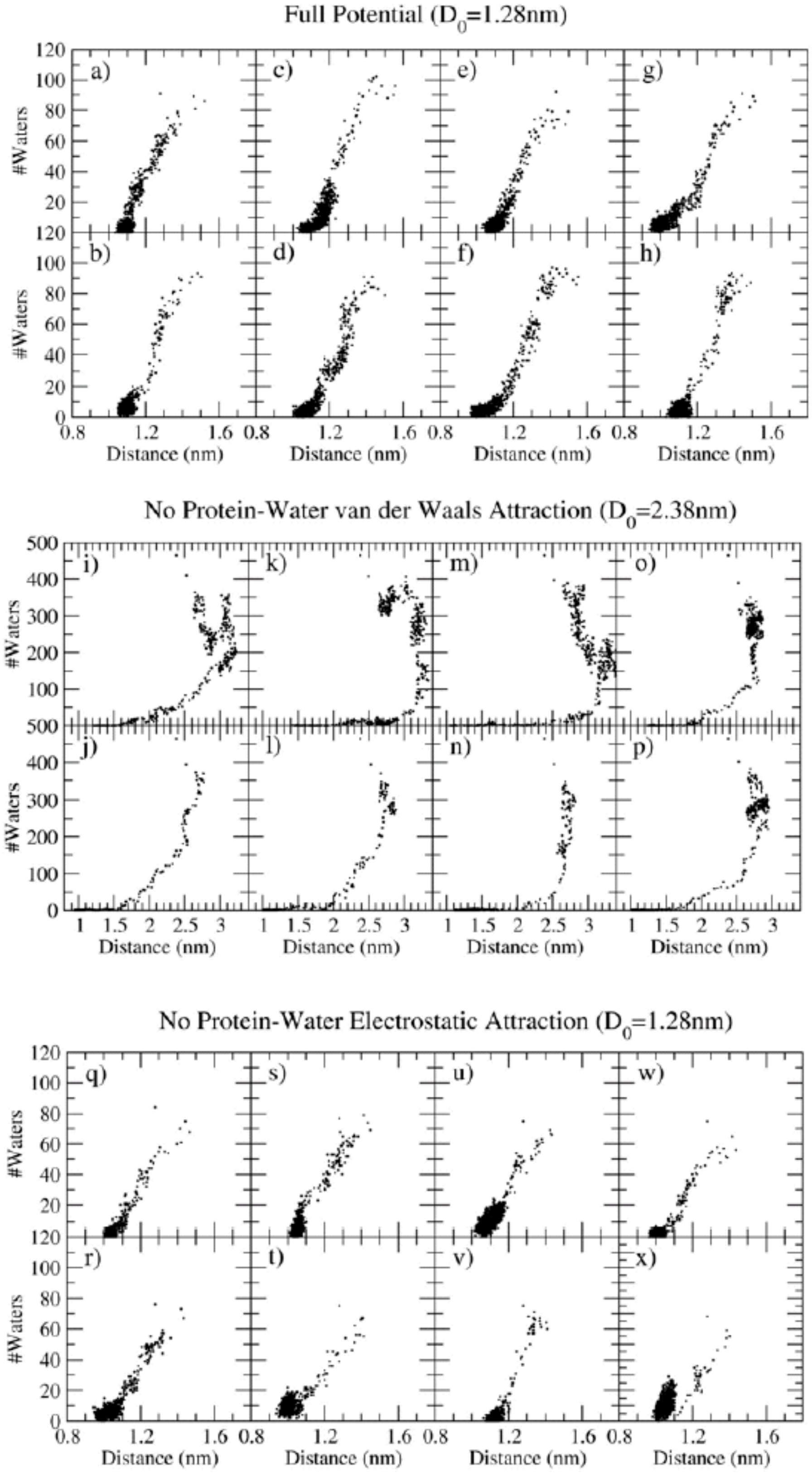
Full Potential (D_0=1.28nm)
a)
b)
c)
d)
e)
f)
g)
h)
#Waters
0
20
40
60
80
100
120
Distance (nm)
0.8
1.2
1.6
No Protein-Water van der Waals Attraction (D_0=2.38nm)
i)
j)
k)
l)
m)
n)
o)
p)
#Waters
0
100
200
300
400
500
Distance (nm)
1
1.5
2
2.5
3
No Protein-Water Electrostatic Attraction (D_0=1.28nm)
q)
r)
s)
t)
u)
v)
w)
x)
#Waters
0
20
40
60
80
100
120
Distance (nm)
0.8
1.2
1.6

Figure 10:

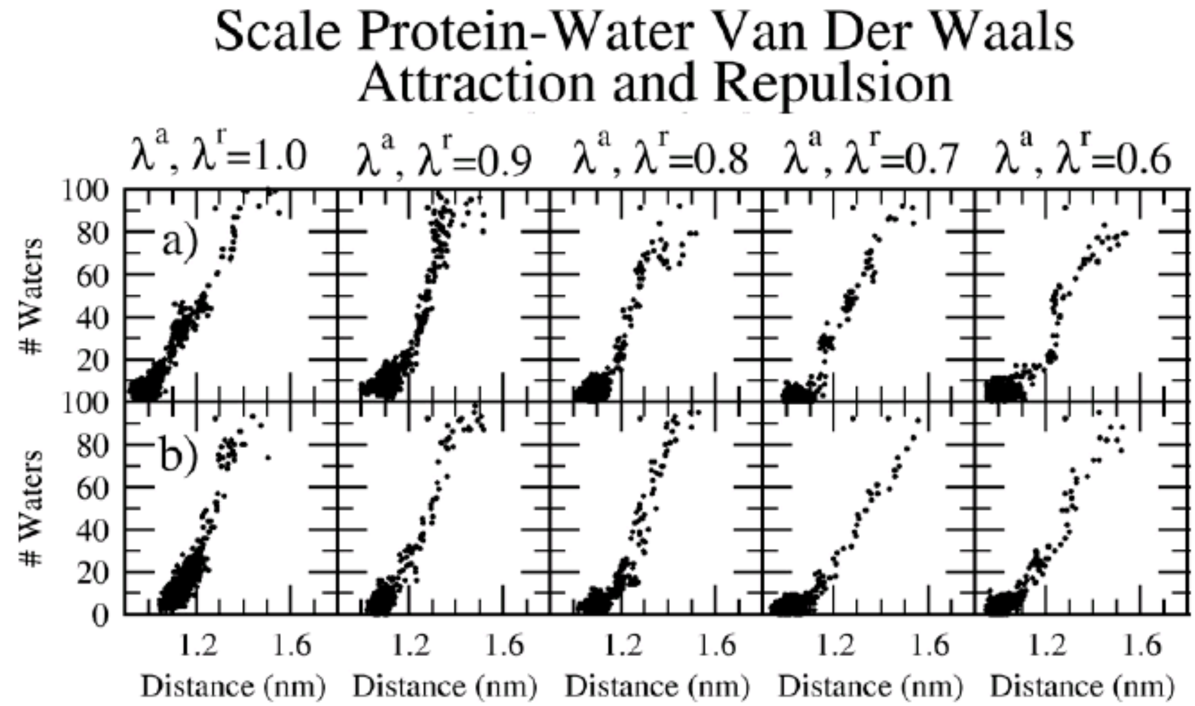
Scale Protein-Water Van Der Waals
Attraction and Repulsion
λ^a, λ^r=1.0
λ^a, λ^r=0.9
λ^a, λ^r=0.8
λ^a, λ^r=0.7
λ^a, λ^r=0.6
a)
b)
Waters
Waters
100
80
60
40
20
100
80
60
40
20
0
1.2
1.6
Distance (nm)